Crystallization and Melting Behaviors of Poly(trimethylene terephthalate)

Jieh-Ming Huang[1,2], Ming-Yih Ju[1], Peter P. Chu[3] and Feng-Chih Chang[1,*]

1. *Institute of Applied Chemistry, National Chiao-Tung University, Hsinchu, Taiwan 30010, R.O.C.*
2. *Department of Chemical Engineering, Van Nung Institute of Technology, Chung-Li, Taiwan 320, R.O.C.*
3. *Department of Chemistry, National Central University, Chung-Li, Taiwan 32001, R.O.C.*

Abstract: The crystallization and melting behaviors of poly(trimethylene terephthalate) (PTT) have been studied by differential scanning calorimetry (DSC), wide-angle X-ray diffraction (WAXD), and solid-state NMR. At certain crystallization temperatures (T_c) for a given time, the isothermally crystallized PTT exhibits two melting endotherms, which is similar to that of PET and PBT. At higher crystallization temperature (T_c = 210 °C), the low-temperature endotherm is related to the melting of the original crystals, while the high-temperature endotherm is associated with the melting of crystals recrystallized during the heating. The peak temperatures of these double-melting endotherms depend on crystallization temperature, crystallization time, and cooling rate from the melt as well as the subsequent heating rate. At a low cooling rate (0.2 °C/min) or a high heating rate (40 °C/min), these two endotherms tend to coalesce into a single endotherm, which is considered as complete melting without reorganization. WAXD results confirm that only one crystal structure exists in the PTT sample regardless of the crystallization conditions even with the appearance of double melting endotherms. The results of NMR reveal that the annealing treatment increases proton spin lattice relaxation time in the rotation frame, $T_{1\rho}^H$, of the PTT. This phenomenon suggests that the mobility of the PTT molecules decreases after the annealing process. The equilibrium melting temperature (T_m^o) determined by the Hoffman-Weeks plot is 248 °C.

Keywords: Poly(trimethylene terephthalate), Melting behavior, Crystallization, Differential scanning calorimetry, Double melting endotherms.

Introduction

Poly(trimethylene terephthalate) (PTT) with three methylene groups in the backbone is a linear aromatic polyester. PTT is obtained by transesterification and polycondensation using trimethylene glycol and terephthalic acid in the melt phase with tetraisopropyl titanate as the catalyst [1-3] that has the following structure:

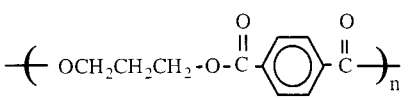

PTT

PTT has been investigated recently as an engineering thermoplastic and as a matrix for fiber-reinforced composites [4,5] due to its attractive mechanical properties and rapid crystallization rate. From a scientific viewpoint, information from PTT coupled with corresponding data from poly(ethylene terephthalate) (PET) and poly(butylene terephthalate) (PBT) make knowledge on this polyester family more complete.

High-resolution solid-state NMR is a powerful and effective tool for studying the molecular structures and molecular dynamics of polymers and its use is growing rapidly [6,7]. In particular, proton spin lattice relaxation time in the rotation frame, $T_{1\rho}^H$, and transverse relaxation time, T_2, were frequently used to provide information on polymer investigations [8]. In a previous paper [9], we reported that both the crystallization temperature and

*To whom all correspondence should be addressed.
Tel: 886-3-5712121 ext. 56502; Fax: 556-3-5723764
E-mail: changfc@cc.nctu.edu.tw

J. Polym. Res. is covered in ISI (CD, D, MS, Q, RC, S), CA, EI, and Polymer Contents.

time affect the relaxation time of polyamide-6 (PA6) in the blend. Furthermore, solid-state NMR can monitor the conformational changes for poly (ethylene terephthalate) (PET) that has been treated at different thermal conditions. It is interesting to compare the relaxation time with crystallinity of polymers by means of solid-state NMR and DSC measurement [10].

Differential scanning calorimetry (DSC) thermogram of PTT shows two melting endotherms. Different crystal structures have been reported to cause the multiple melting endotherms for isotactic poly (propylene) and poly(vinylidene fluoride) [11,12]. Simultaneous melting and recrystallization has been found as the origin of double melting for PET [13], nylon 66 [14,15], and isotactic polystyrene [16]. Lee et al. [17,18] has reported that the double endotherms of PEEK are resulted from the sum of four contributions: partial melting of the original crystals, their recrystallization, melting of recrystallized crystals, and melting of core crystals. Similar to PEEK, PTT also shows double melting endotherms in the DSC thermogram but so far no detailed data has been reported on the melting behaviors of PTT. The purpose of this paper is to investigate the nonisothermal and isothermal crystallization of PTT.

Experimental

1. Materials

Poly(trimethylene terephthalate) (PTT) was obtained from the Shinkong Synthetic Fibers Co. (Taiwan) in the form of pellets. The intrinsic viscosity (I.V.) of PTT in a 60/40 mixed solvent of phenol and tetrachloroethane at 25 °C was measured to be 0.80 dL/g.

2. High-resolution solid-state NMR measurements

High-resolution solid-state ^{13}C NMR experiments were carried out on a Bruker DSX-300 spectrometer operating at resonance frequencies of 300.13 and 75.475 MHz for ^{1}H and ^{13}C, respectively. ^{13}C CP/MAS NMR spectra were measured by the following conditions: 90° pulse width, 3.9 μs; pulse delay time, 3 s; acquisition time, 30 ms. All NMR spectra were recorded with broad band proton decoupling (ν_1 = 64 KHz), and a conventional cross-polarization pulse sequence. The magic-angle sample spinning (MAS) rate of 4 KHz was used to avoid overlapping resonance lines. Proton spin-lattice relaxation times in the rotating frame ($T_{1\rho}^{H}$) were measured indirectly via carbon observation with a spin lock pulse prior to cross-polarization. Data acquisitions were performed with ^{1}H decoupling (ν_1 = 64 kHz), using spin-lock times ranging from 0.2 to 12 ms. The contact time was 1.5 ms.

3. Wide-angle X-ray diffraction

X-ray diffraction (XRD) was performed on the PTT samples prepared as thin discs in the DSC. The XRD studies were conducted on an INEL MPD-diffractometer using the Ni-filtered Cu K_α (λ = 1.541 Å) radiation at 30 mA, 40 KV, and 2θ ranging from 5° to 35°.

4. Differential scanning calorimetry measurements

The glass transition temperature (T_g) of PTT was determined using a Perkin-Elmer DSC-7. About 4 mg sample of PTT was placed in the DSC pan and heated above the melting temperature for 5 min. The sample was then quenched into a liquid nitrogen bath. Upon reheating at 10 °C/min, an inflection point as the glass transition temperature was observed. For the equilibrium melting temperature measurement, the PTT sample was melted at 260 °C for 5 min under a nitrogen atmosphere to erase previous thermal histories. The sample was subsequently quenched at a rate of 300 °C/min to the desired crystallization temperature (T_c). After crystallization for 24 h, the sample was immediately heated up from T_c to 270 °C at a heating rate of 10 °C/min. The peak temperature of the endotherm was considered as the melting point of the sample. For nonisothermal crystallization study, the PTT samples were melted at 260 °C for 5 min and then cooled from 260 to 30 °C at various rates (0.2 to 80 °C/min). Sub-sequently, the samples were reheated from room temperature to 260 °C at a heating rate of 10 °C/min. The crystallinity of the samples was obtained from DSC data. From the measured heat of fusion ΔH_m an apparent degree of crystallinity is calculated as follows:

$$X_{DSC} = \Delta H_m/\Delta H^\circ \quad (1)$$

where ΔH° is the heat of fusion of fully crystalline PTT. A value of 30 kJ/mol has been adopted for ΔH° [19].

Results and Discussion

1. High-resolution solid-state NMR studies

^{13}C CP/MAS NMR spectrum of PTT is shown in Figure 1. The combination of dipolar decoupling and magic-angle spinning (MAS) results in sufficiently high resolution to resolve the carbonyl carbon (δ_0 = 165.5 ppm), aromatic carbons (130.3 and 133.7 ppm), and methylene carbons (62.3 and 27.6 ppm). The magnetization decay curves of the ^{13}C

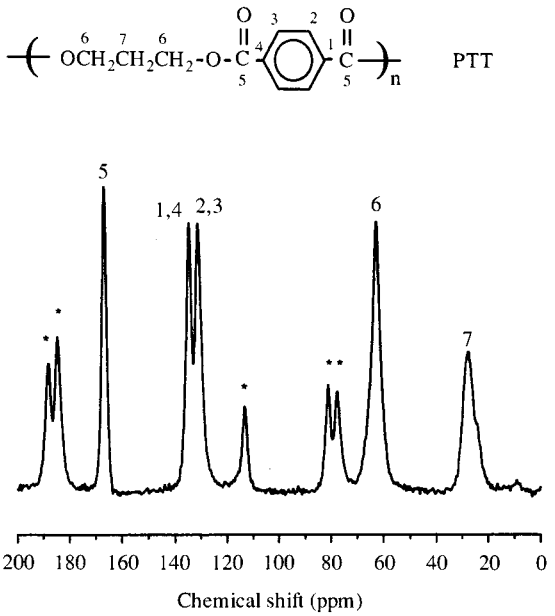

Figure 1. ^{13}C CP/MAS NMR spectrum of PTT. Asterisks denote spinning sidebands.

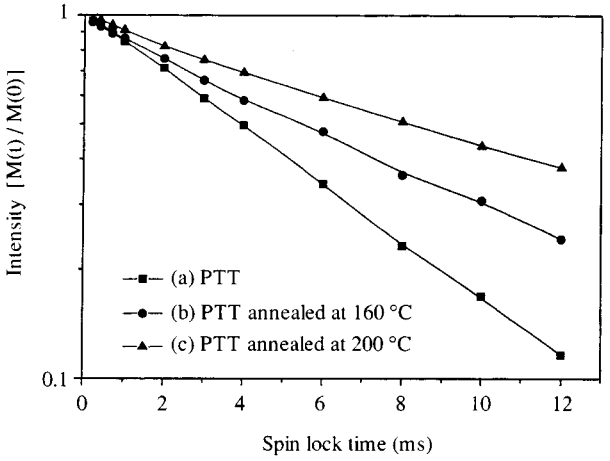

Figure 2. Semi-logarithmic plots of the magnetization intensity of methylene (62.3 ppm) as a function of spin-lock time for PTT annealed at different temperetures.

signal of methylene carbon (62.3 ppm) for the virgin PTT and the annealed PTT are plotted on a logarithmic scale vs proton spin-lock time, as shown in Figure 2. From the Figure, proton spin lattice relaxation time in the rotation frame $T_{1\rho}^H$ can be calculated from the slope of the line, and the results are summarized in Table I. It is well known that annealing treatment has a pronounced effect on the physical properties of polymers. Particularly, annealing above T_g causes densification and formation crystalline domains. The $T_{1\rho}^H$ value (62.3 ppm) increases from 6.12 ms for the virgin PTT to 14.40 ms for the PTT sample annealed at 200 °C for 1h. The $T_{1\rho}^H$ data shown in Table I indicates that the relaxation time in the rotating-frame is sensitive to the thermal histories of the PTT samples. It is evident that higher annealing temperature results in longer $T_{1\rho}^H$ value. The increased $T_{1\rho}^H$ value of the methylene-carbon is also a result of increasing crystallinity, which further inhibits motion in the amorphous region. This means that the annealing treatment increases the relaxation time in the rotating frame and reduces the mobility of the PTT molecules.

Table I. $T_{1\rho}^H$ values of PTT at various annealing temperatures for 1 h.

Annealing temperature (°C)	$T_{1\rho}^H$ (ms)			
	62.3 (ppm)	130.3 (ppm)	133.7 (ppm)	165.5 (ppm)
virgin PTT	6.12	5.68	5.50	6.22
160	10.80	8.66	9.78	9.20
200	14.40	16.54	14.24	14.87

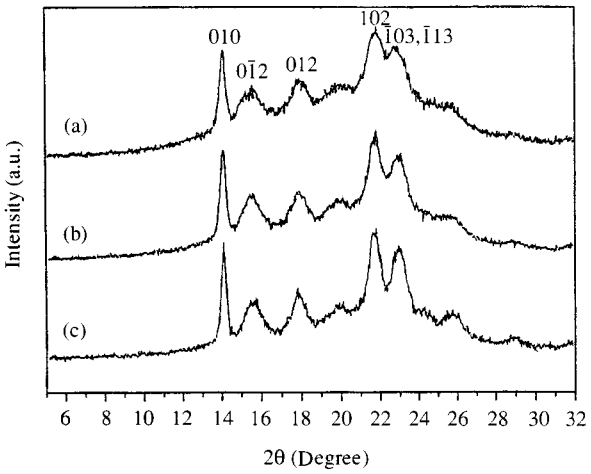

Figure 3. WAXD patterns for PTT cooled to room temperature at different cooling rates: (a) -60 °C/min, (b) -10 °C/min, and (c) -0.2 °C/min.

2. Wide-angle X-ray diffraction (WAXD)

The X-ray diffraction patterns for samples prepared in the DSC at different cooling rates (60, 10, and 0.2 °C/min) from the melt are shown in Figure 3. The intensity of scattering is plotted as a function of 2θ and the crystal lattice is also designated [20]. The result in Figure 3 shows that the breadth (half-width) of the diffraction peak becomes sharper with decreasing cooling rate from the melt, indicating that the size of the crystallite becomes larger and the spherulite becomes more complete. Therefore, the long-period of the annealed specimen would increase as the cooling rate is decreased. However, all these PTT samples exhibit similar diffraction patterns, implying that the crystal lattices

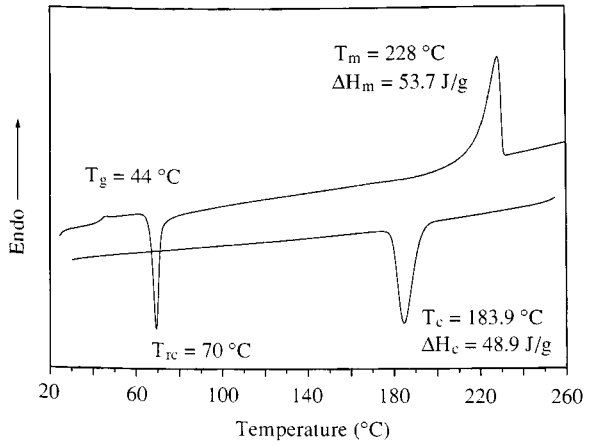

Figure 4. DSC heating trace for PTT quenched from the melt and the subsequent cooling trace. Heating and cooling rates are 10 °C/min.

of these PTT samples do not change with different cooling rates. These PTT samples may show one or two melting endotherms in DSC scan but have the same WAXD patterns. This indicates that only one crystal structure exists in these PTT samples regardless of the crystallization conditions.

3. Nonisothermal crystallization behavior

DSC heating trace for PTT quenched from the melt and the subsequent cooling trace are shown in Figure 4. It is evident that there is a distinct glass transition temperature (T_g = 44 °C), an exothermic recrystallization peak (T_{rc} = 70 °C), and an endothermic melting peak (T_m = 228 °C) in the heating scan. The recrystallization exotherm is due to the rapid cooling of the melt specimen into liquid nitrogen, making the full crystallization difficult. From the subsequent cooling scan (10 °C/min), there is a crystallization peak T_c at 183.9 °C. The measured glass transition temperature T_g = 44 °C is very close to T_g = 45 °C reported by Gonzales et al. [2] and T_g = 42 °C reported by Pyda et al. [19]. The DSC heating scans for PTT samples, which were cooled at different rates from the melt to room temperature, are shown in Figure 5. The specimen prepared from the lowest cooling rate (0.2 °C/min) gives only one major endotherm with a small shoulder on the high temperature side. An apparent splitting of the main peak first appears when the cooling rate is 0.4 °C/min. When the cooling rates are higher than 0.4 °C/min, the melting behavior is characterized by two distinct endotherms. Furthermore, the low-temperature endotherm T_m1 decreases its peak temperature and its heat of fusion with increasing cooling rates. All of the heating scans are conducted at a rate of 10 °C/min. From Figure 5(b), one can see that the peak width of the high-temperature endotherm T_m2 increases slightly with the increase of the cooling rate from the melt, implying that the distribution of crystal sizes increases as the cooling rate is faster. The effects of cooling rate on the melting peaks show that two melting endotherms appear for the samples crystallized with the intermediate cooling rates, while only one melting endotherm presents for the higher cooling rate. Since cooling rate increases further, there is no sufficient time for specimen to crystallize during cooling scan, therefore, only one melting endotherm T_m2 indicating the melting of the primary crystals.

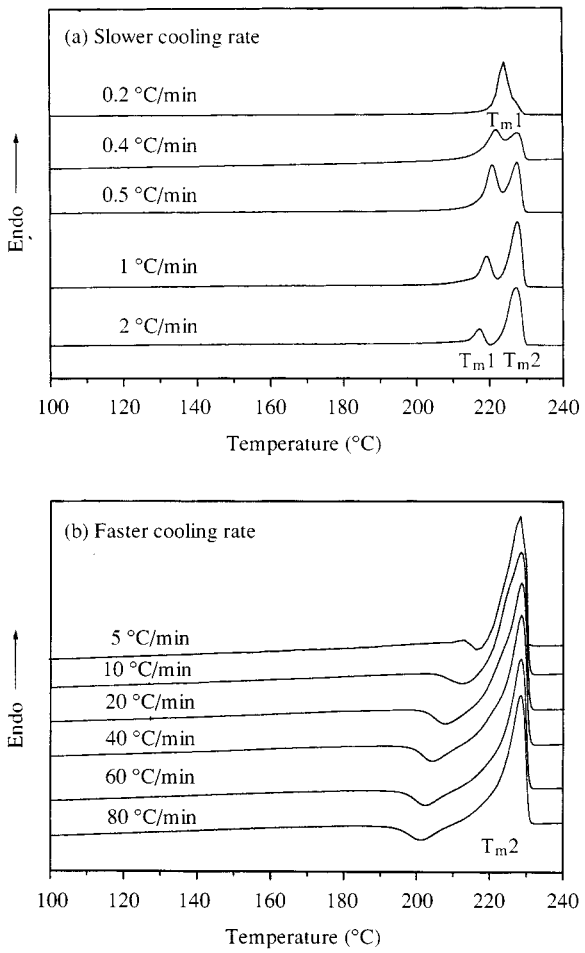

Figure 5. DSC heating traces for PTT cooled to room temperature with different rates: (a) slower and (b) faster cooling rate.

The peak temperatures in Figure 5 are plotted against logarithmic cooling rate as shown in Figure 6. For these two peak temperatures, T_m1 shows a nearly linear relationship with the logarithm of the DSC cooling rate. A similar result has also been reported for poly(butylene terephthalate) (PBT) [21]. The results of the nonisothermal crystallization determined from DSC are summarized in Table II, where the heat of exotherm (ΔH_c) decreases with

Table II. Results of nonisothermal crystallization.

Cooling rate (°C/min)	Crystallization			Melting			Crystallinity
	Onse (°C)	Peak (°C)	ΔH_c (J/g)	T_m1 (°C)	T_m2 (°C)	ΔH_m (J/g)	X_{DSC} (%)
0.2	212.4	211.9	65.7	224.1	–	72.41	49.7
0.5	211.6	208.0	61.8	221.0	227.5	65.82	45.2
1	208.5	204.0	58.1	219.5	227.5	62.21	42.7
2	205.1	200.2	56.6	216.5	227.6	59.04	40.5
5	198.4	191.2	51.4	212	227.3	56.08	38.5
10	192.5	183.9	48.9	–	228.5	54.32	37.3
20	185.0	175.3	46.6	–	228.7	54.0	37.1
40	176.6	163.4	45.8	–	228.6	53.82	37.0
60	169.7	153.7	44.9	–	228.5	53.78	37.0
80	164.1	144.8	43.8	–	228.8	53.64	36.8

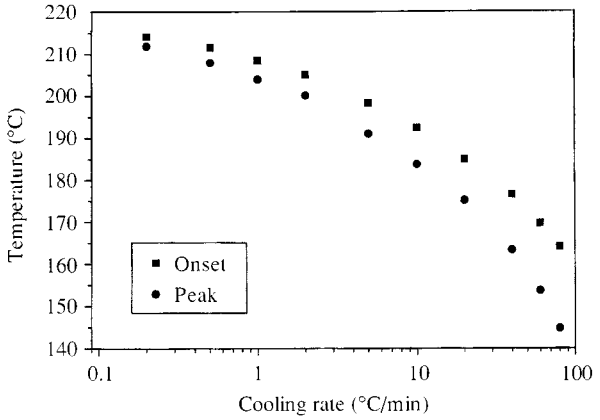

Figure 7. Onset and the peak of the crystallization exotherm as a function of cooling rate.

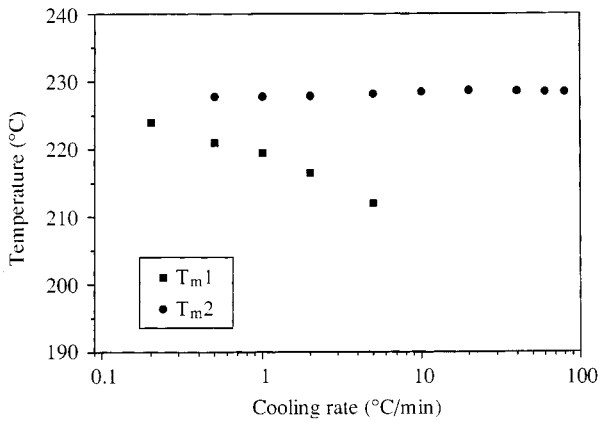

Figure 6. T_m1 and T_m2 of PTT as a function of cooling rate.

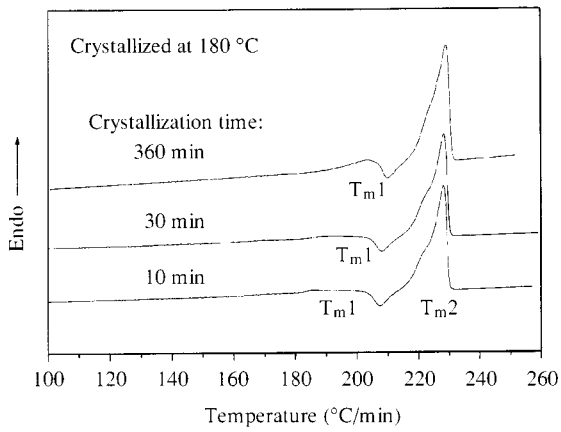

Figure 8. DSC traces of PTT crystallized at 180 °C for different periods of time.

increasing cooling rate as would be expected. Moreover, both the onset and peak temperatures of the crystallization depend on the cooling rate as shown in Figure 7. It can be seen that both the peak onset and peak temperatures of crystallization show the same trend, i.e., they occur at lower temperatures as the cooling rate is increased. Low crystallization temperature leads to relatively thin crystals and results in relatively low melting point. One can see that the difference between the peak onset and peak maximum also increases with increasing cooling rate. Thus, the breadth of the crystalline distribution increases with increasing cooling rate. This result is consistent with the WAXD patterns (see Figure 3), where the peak width is broader at higher cooling rate. Furthermore, the degree of crystallinity decreases when the cooling rate is increased, as shown in Table II.

4. Effect of crystallization time

Figure 8 shows the DSC heating curves of the PTT samples isothermally crystallized at 180 °C for different periods of time. A small endothermic peak appears just above 180 °C when the sample is subjected to the crystallization of 10 min. In addition, this low-temperature melting peak (T_m1) shifts toward high temperature and increases the heat of fusion with the increase of the crystallization time. However, the high-temperature endotherm locating at ca. 228 °C appears to be independent of the crystallization time. The appearance of low-temperature endotherm during crystallization is associated with the formation of imperfect crystals which depend on crystallization temperature and crystallization time. For comparison, DSC heating traces of PTT isothermally crystallized at 210 °C from 10 to 360 min are shown in Figure 9 and the results are also tabulated in Table III. When the specimen was crystallized for 10 min, the low-temperature endotherm appears just before T_m2 and the area of T_m1 increases rapidly with crystallization time. The general trends for the T_m1 are that both melting heat and peak temperature increase gradually with the increase of crystallization time. After long-time crystallization (360 min) the T_m2 endothermic peak

Table III. The effects of heating rate and crystallization time on the thermal data for PTT crystallized at 210 °C.

Cooling rate (°C/min)	Crystallization time (min)	Melting		Crystallinity
		T_m2 (°C)	ΔH_m (J/g)	X_{DSC} (%)
5	60	228.8	57.2	39.3
10	60	228.3	56.8	39.0
20	60	228.0	56.5	38.7
40	60	–	55.9	38.3
10	10	227.8	53.1	36.5
10	60	228.3	56.8	39.0
10	360	–	61.6	42.3

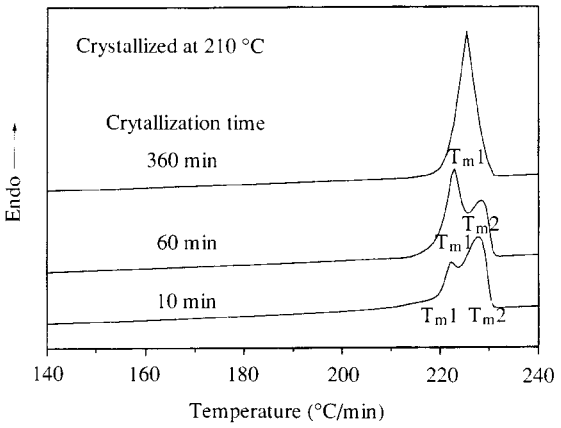

Figure 9. DSC traces of PTT crystallized at 210 °C for different periods of time.

diminishes completely and eventually gives only the T_m1 endotherm. Furthermore, T_m1 moves to a higher temperature (225.5 °C), which is 3 °C higher than that of the low- temperature endotherm produced by a 10 min crystallization. The increase in peak temperature and heat of fusion of the T_m1 endotherm is an indication of gradual perfection in crystallization and that the T_m2 endotherm is associated with the melting of the recrystallized crystals. A similar result has been reported for PET [13] and nylon 6,6 [16,17]. Roberts et al. [13] reported that annealing causes an increase in the melting temperature of all crystals. For those melted crystals, the driving force for recrystallization is lower because of a lower degree of supercooling. The net effect is that, the melting temperature for the crystalline material as a whole increase, the amount of material which has sufficient time to recrystallize decreases.

5. Effect of heating rate

In order to confirm the claim that recrystallization is the cause of the double melting behavior of the PTT, DSC heating traces for PTT isothermally crystallized at 210 °C for 1 h with different rates

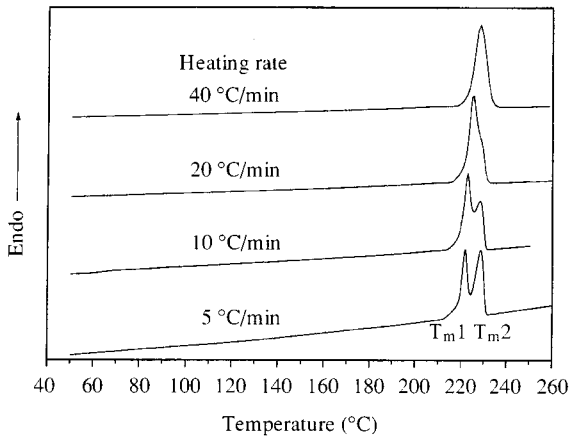

Figure 10. DSC traces of PTT crystallized at 210 °C for 1 h at various heating rates.

are shown in Figure 10. As the heating rate is increased, the low-temperature melting endotherm T_m1 increases in size (relative to T_m2) and peak temperature, while the high-temperature melting endotherm T_m2 decreased in size and peak temperature. However, the total heat of fusion does not change drastically with different heating rates as shown in Table III. A similar behavior was reported for PEEK isothermally crystallized at 220 °C [17]. When the heating rate is increased, the time allowed for recrystallization decreases and thus results in a smaller high-temperature melting endotherm and a larger low-temperature endotherm. It can be seen in Figure 10 that at a heating rate of 40 °C/min, the two distinct melting endotherms appear to coalesce into a single endotherm due to a lower supercooling and less time allowed for recrystallization. It is noteworthy that the breadth of the coalesced endotherm is broader at this higher heating rate. From this result, the heating rate of 40 °C/min appears to be enough to minimize the reorganization during the heating in the DSC. As the heating rate exceeds 40 °C/min, the peak temperature of the merged single endotherm shifts to higher temperature. This may be due to the lower thermal conductivity of the polymer.

6. Equilibrium melting temperature

Figure 11 shows the typical melting behavior of PTT isothermally crystallized from 200 to 219 °C for 24 h. The variation of the observed melting temperature with the crystallization temperature is shown in Figure 12. In the range of T_c investigated, the T_m of PTT increases almost linearly with T_c according to the Hoffman-Weeks equation [22]:

$$T_m = T_c / \gamma + T_m^\circ (1 - 1/\gamma) \quad (2)$$

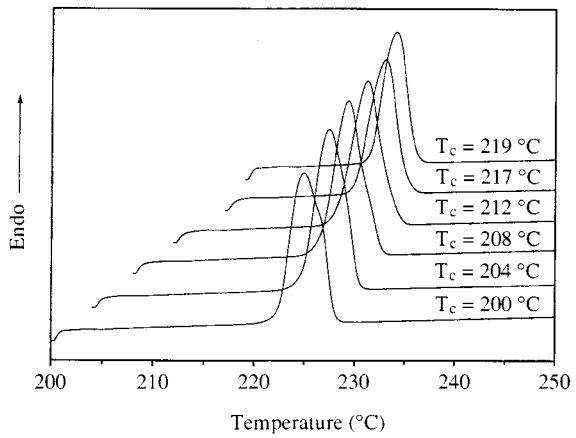

Figure 11. DSC heating traces of PTT crystallized at various temperatures for 24 h (heating rate = 10 °C/min).

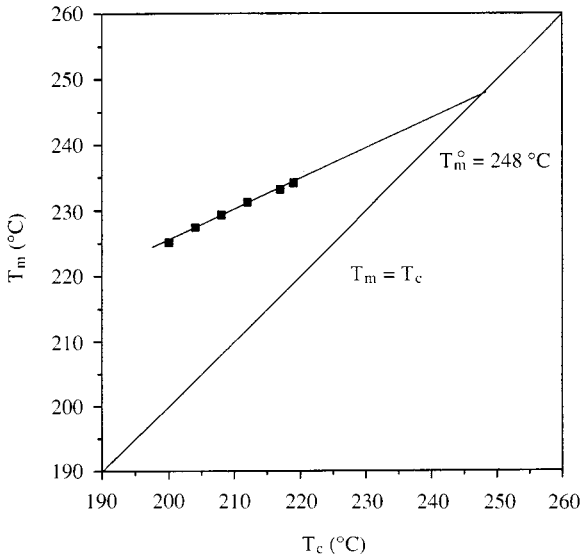

Figure 12. Hoffman-Weeks plot for isothermally crystallized PTT (24-h crystallization).

where T_m and T_m^o are the experimental melting temperature and equilibrium melting temperature of PTT. γ is the ratio of the lamellar thickness to the critical lamellar thickness. According to Eq.(2) the equilibrium melting temperature can be determined from the intersection of the extrapolated T_m value with the line defined by $T_m = T_c$. The value of T_m^o obtained by this method is 248 °C. When processing with quantitative analysis of the crystallization behavior, the equilibrium melting temperature is important since the thermodynamic parameters are very sensitive to the value of T_m^o.

Conclusions

In isothermal crystallization experiments, the double melting behavior of PTT can be attributed to crystallite reorganization on heating. The peak temperatures of these two melting endotherms depend on the annealing temperature and the subsequent heating rate. For a long-time annealing or a high heating rate (40 °C/min), these two endotherms tend to coalesce into a single peak. The coalesced endotherm represents the complete melting of the original crystals without reorganization. The results of solid-state NMR experiments suggest that the annealing treatment increases the relaxation time $T_{1\rho}{}^H$ and decreases the mobility of the PTT moleculars. This is associated with the formation of crystallites during the annealing process. Nonisothermal crystallization results show that T_m1 appears a nearly linear relationship with the logarithmic DSC cooling rate, whereas T_m2 seems independent of the cooling rate. Furthermore, these two melting endotherms of PTT in the subsequent heating scan coalesce into one peak for the lowest cooling rate (0.2 °C/min). However, WAXD patterns of the PTT samples confirm that only one crystal structure exists regardless of the crystallization conditions.

Acknowledgment

The financial support by National Science Council under grant NSC87-2216-E-009-006 is greatly appreciated. The authors are also indebted to Shinkong Synthetic Fibres Co. for supporting poly (trimethylene terephthalate) samples.

References

1. T. H. Ng and H. L. Williams, *Makromol. Chem.*, **182**, 3323 (1981).
2. C. C. Gonzalez, J. M. Perena and A. Bello, *J. Polym. Sci., Polym. Phys. Ed.*, **26**, 1397 (1988).
3. T. Imamura, T. Sato and T. Matsumoto, Jpn. Pat. 08, 232,117 (1996).
4. K. Dangayach, H. Chuah, W. Gergen, P. Dalton and F. Smith, *Plastics-Saving Planet Earth*, 55th ANTEC Proc., 2097 (1997).
5. K. Tsumashima, and M. Suzuki, Jpn. Pat. 08,104,763 (1996).
6. Z. Gao, A. Molnar, F. G. Morin and A. Eisenberg, *Macromolecules*, **25**, 6460 (1992).
7. V. T. McBrierty, D. C. Douglass and T. K. Kwei, *Magn. Reson. in Chem.*, **32**, 853 (1994).
8. D. L. Vanderhar and J. D. Barnes, *Macromolecules*, **27**, 2826 (1994).
9. P. P. Chu, J. M. Huang, H. D. Wu, C. R. Chiang and F. C. Chang, *J. Polym. Sci., Polym. Phys. Ed.*, **37**, 1155 (1999).
10. J. M. Huang, P. P. Chu and F. C. Chang, *Polymer*, **41**, 1741 (2000).
11. R. J. Samuels, *J. Polym. Sci., Polym. Phys. Ed.*, **13**, 1417 (1975).

12. W. M. Prest and D. J. Luca, *J. Appl. Phys.*, **46**, 4136 (1975).
13. R. C. Roberts, *Polymer*, **10**, 17 (1969).
14. G. E. Sweet and J. P. Bell, *J. Polym. Sci., Polym. Phys. Ed.*, **10**, 273 (1972).
15. M. Todoki and T. Kawaguchi, *J. Polym. Sci., Polym. Phys. Ed.*, **15**, 1067 (1977).
16. J. Boon, G. Challa and D.W. Krevelen, *J. Polym. Sci., Polym. Phys. Ed.*, **6**, 1791 (1968).
17. Y. Lee and R. S. Porter, *Macromolecules*, **20**, 1336 (1987).
18. Y. Lee, R. S. Porter and J. S. Lin, *Macromolecules*, **22**, 1756 (1989).
19. M. Pyda, A. Boller, J. Grebowicz, H. Chuah, V. Lebedev and B. Wunderlich, *J. Polym. Sci., Polym. Phys. Ed.*, **36**, 2499 (1998).
20. S. Peres, P. D. Suzie, J. F. Revol and F. Brisse, *Polymer*, **20**, 419 (1979).
21. R. E. Robertson and M. E. Michols, *J. Polym. Sci., Polym. Phys. Ed.*, **30**, 755 (1992).
22. J. D. Hoffman and J. J. Weeks, *J. Chem. Phys.*, **42**, 4301 (1965).